


# Lamin A/C negatively regulated by miR-124-3p modulates apoptosis of vascular smooth muscle cells during cyclic stretch application in rats

Han Bao<sup>1</sup> | Hai-Peng Li<sup>1</sup> | Qian Shi<sup>1</sup> | Kai Huang<sup>1</sup> | Xiao-Hu Chen<sup>1</sup> | Yuan-Xiu Chen<sup>1</sup> | Yue Han<sup>1</sup> | Qian Xiao<sup>1</sup> | Qing-Ping Yao<sup>1</sup> | Ying-Xin Qi<sup>1,2,3</sup> 

<sup>1</sup>Institute of Mechanobiology & Medical Engineering, School of Life Sciences & Biotechnology, Shanghai Jiao Tong University, Shanghai, China

<sup>2</sup>Key Laboratory for Biomechanics and Mechanobiology of Ministry of Education, School of Biological Science and Medical Engineering, Beihang University, Beijing, China

<sup>3</sup>Beijing Advanced Innovation Center for Biomedical Engineering, Beihang University, Beijing, China

## Correspondence

Ying-Xin Qi, Institute of Mechanobiology & Medical Engineering, School of Life Sciences & Biotechnology, Shanghai Jiao Tong University, Minhang, Shanghai, China.

Email: qiyx@sjtu.edu.cn

## Funding information

National Natural Science Foundation of China, Grant/Award Number: 11572199 and 11625209

## Abstract

**Aim:** Apoptosis of vascular smooth muscle cells (VSMCs) influenced by abnormal cyclic stretch is crucial for vascular remodelling during hypertension. Lamin A/C, a nuclear envelope protein, is mechano-responsive, but the role of lamin A/C in VSMC apoptosis is still unclear.

**Methods:** FX-5000T Strain Unit provided cyclic stretch (CS) *in vitro*. Annexin V/PI and cleaved Caspase 3 ELISA detected apoptosis. qPCR was used to investigate the expression of miR-124-3p and a luciferase reporter assay was used to evaluate the ability of miR-124-3p binding to the Lmna 3'UTR. Protein changes of lamin A/C and relevant molecules were detected using western blot. Ingenuity Pathway Analysis and Protein/DNA array detected the potential transcription factors. Renal hypertensive rats verified these changes.

**Results:** High cyclic stretch (15%-CS) induced VSMC apoptosis and repressed lamin A/C expressions compared with normal (5%-CS) control. Downregulation of lamin A/C enhanced VSMC apoptosis. In addition, 15%-CS had no significant effect on mRNA expression of Lmna, and lamin A/C degradation was not induced by autophagy. 15%-CS elevated miR-124-3p bound to the 3'UTR of Lmna and negatively regulated protein expression of lamin A/C. Similar changes occurred in renal hypertensive rats compared with sham controls. Lamin A/C repression affected activity of TP53, CREB1, MYC, STAT1/5/6 and JUN, which may in turn affect apoptosis.

**Conclusion:** Our data suggested that the decreased expression of lamin A/C upon abnormal cyclic stretch and hypertension may induce VSMC apoptosis. These mechano-responsive factors play important roles in VSMC apoptosis and might be novel therapeutic targets for vascular remodelling in hypertension.

## KEYWORDS

apoptosis, cyclic stretch, lamin A/C, mechanobiology, vascular smooth muscle cells

## 1 | INTRODUCTION

Vascular smooth muscle cells (VSMCs) are dominant cellular constituents of arteries and are critical determinants of vascular disease.<sup>1</sup> In hypertension, VSMCs undergo significant dysfunction, which increases the ratio of vascular wall thickness to luminal diameter, and enhances the vascular remodelling.<sup>2</sup> VSMC apoptosis has been shown to be an important process in remodelling arteries during hypertensive circumstances.<sup>3</sup> In the process of artery remodelling during systemic hypertension, VSMC apoptosis is promoted, and extracellular collagen synthesis and degradation are imbalanced, leading to an excessive deposition of collagen in the vascular wall.<sup>4</sup>

During hypertension, mechanical cyclic stretch, defined as repetitive deformation of the cells as a vessel wall rhythmically distends and relaxes with the cardiac cycle, is significantly increased.<sup>5</sup> Various studies have revealed that this pathologically changed force plays crucial roles in vascular remodelling diseases associated with hypertension.<sup>6</sup> Mechanical cyclic stretch induces phenotype switching, proliferation,<sup>7</sup> apoptosis<sup>8</sup> and migration<sup>9</sup> of VSMCs. Many mechano-responsive signalling pathways have been indicated to be influenced by cyclic stretch, including the PI3K/Akt,<sup>10</sup> PKC,<sup>11</sup> NFκB,<sup>12</sup> Rho family GTPases<sup>13</sup> and MAPK pathways.<sup>14</sup> In addition, cytoskeletal proteins in both the cytoplasm and nucleus are also responsive to varying degrees of cyclic stretch. For example, cyclic stretch induces realignment and rearrangement of microfilaments<sup>15</sup> and reorientation of microtubules and intermediate filaments.<sup>16</sup> Our recent work shows that lamin A and emerin, important cytoskeletal proteins in the nucleus, are responsive to both cyclic stretch and shear stress.<sup>7,17</sup>

Lamins are nuclear intermediate filament proteins and constitute structural components of the nuclear lamina, which is a protein network underlying the inner nuclear membrane that determines nuclear shape and size.<sup>18</sup> Two types of lamins are found in mammalian cells: A-type lamins, including lamin A, C, AΔ10 and C2, are encoded by a single gene (*Lmna*) and are developmentally regulated and expressed in differentiated cells; B-type lamins, including lamin B1 and B2/B3, are encoded by two distinct genes and are constitutively expressed in all cells.<sup>19</sup> In mechano-responsive processes, lamin A and C are stress-sensitive molecules that have been widely studied. For example, when BEAS-2b cells are subjected to 18% equibiaxial stretch, the expression of lamin A and its ratio to lamin B expression both increase significantly, which then changes the compliance of nuclei.<sup>20</sup>

Although studies have proven that different kinds of mechanical stimuli regulate lamin A/C, the detailed mechanisms involved in these processes are still unclear. Transcriptional regulation, protein synthesis, degradation and rearrangement may all participate in varying the expression of lamin

A/C. Our preliminary experiment indicated that inhibition of the ubiquitin degradation pathway partially reversed the repression of lamin A/C induced by abnormal cyclic stretch. However, this reversal process was not complete, which suggested that there are other regulatory mechanisms that affect the expression of lamin A/C. Here, we tried to demonstrate the mechanism of the altered expression of lamin A/C under abnormal cyclic stretch and to further detect the role of this altered expression in VSMC apoptosis.

In this study, the roles of miRNA regulation and protein degradation induced by autophagy were first explored under cyclic stretch application. Then, the role of repressed lamin A/C in the apoptosis process of VSMCs was demonstrated. This study may provide a new insight into understanding the mechanism of VSMC dysfunction in hypertension, and may provide a potential target to maintain VSMC homeostasis in physiologically and pathologically.

## 2 | RESULTS

### 2.1 | Pathological cyclic stretch represses the expression of Lamin A/C and induces the apoptosis of VSMCs

Mechanical circumferential stress is significantly increased by high blood pressure which causes more intense deformation of the elastic blood vessels.<sup>21</sup> Using an FX-5000T Strain Unit system, different magnitudes of cyclic stretch were applied to VSMCs in vitro.

Compared with 5% cyclic stretch (physiological stretch to mimic normal tension), 15% cyclic stretch (pathological stretch to mimic hypertension) significantly increased the apoptosis of VSMCs, which was detected using both Annexin V/PI staining (Figure 1A) and cleaved Caspase 3 ELISA (Figure 1B). In addition, the protein expressions of lamin A/C were studied after the cells were subjected to different levels of cyclic stretch. Compared with 5%-CS, 15%-CS decreased the expression of lamin A (at 6, 12, and 24 hours) (Figure 1C) and lamin C (at 24 hours but not at 6 or 12 hours) (Figure 1D).

These results implied that pathological elevated cyclic stretch induced VSMC apoptosis and repressed lamin A/C protein expression.

### 2.2 | Repressed expression of lamin A/C induces apoptosis of VSMCs

Because the altered expressions of lamin A/C were accompanied by changes in apoptosis under pathological cyclic stretch, we detected whether lamin A/C participated in the modulation of apoptosis.

Under the static conditions, specific siRNA was used to specifically decrease the expression of lamin A/C (Figure

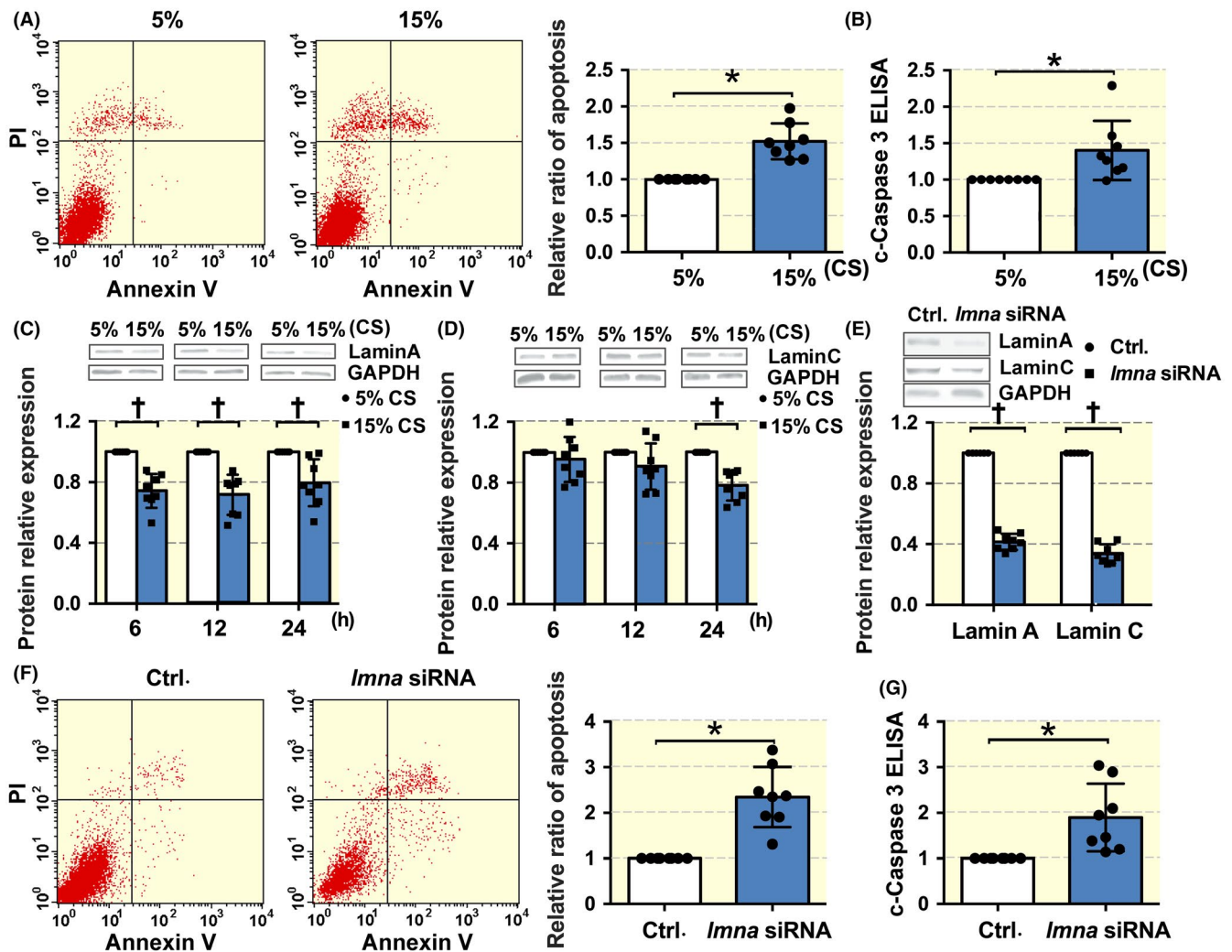


**FIGURE 1** Cyclic stretch (CS) modulated the expression of lamin A/C, which participates in the apoptosis of VSMCs in vitro. A, A cyclic stretch level of 15% increased VSMC apoptosis in comparison with a level of 5%, as detected with AnnexinV-FITC/PI staining. B, A cyclic stretch level of 15% increased VSMC apoptosis in comparison with a level of 5%, as detected using cleaved Caspase 3 analysis. C and D, A cyclic stretch level of 15% decreased the expression of lamin A and lamin C in comparison with a level of 5%. E, Lamin A/C targeted RNA interference (RNAi) markedly suppressed the expression of both lamin A and lamin C, under the static condition. F, Lamin A/C targeted siRNA increased VSMC apoptosis, as detected with AnnexinV-FITC/PI staining. G, Lamin A/C targeted siRNA increased VSMC apoptosis, as detected using cleaved Caspase 3 analysis. Non-silencing siRNA with no known homology to rat genes was synthesized as a negative control (NC). The values represent the mean  $\pm$  SD. \* $P < .05$ ,  $\dagger P < .01$  vs. control. The control value (for A-D, 5%-CS was used as the control, and for E-G, the control was the siRNA negative control) was standardized to 1 (n = 8)

1E). Lamin A/C knockdown significantly increased the apoptosis of VSMCs under static conditions (Figure 1F,G).

Together, our results regarding lamin A/C expression and VSMC apoptosis under stretch application suggested that the repression of lamin A/C induced by pathological cyclic stretch may contribute to the regulation of VSMC apoptosis.

### 2.3 | Decreased expression of lamin A/C is not regulated by transcription or autophagy

Since the protein expressions of lamin A/C were decreased under 15%-CS, we then explored the potential mechanisms in this process. Although our preliminary experiment revealed

a partial effect of the ubiquitin degradation pathway in this process,<sup>7</sup> the detailed regulatory mechanisms of the expression of lamin A/C were further detected.

First, we detected the effects of different levels of cyclic stretch on the expression of *Lmna*, the mRNA of lamin A/C. The results revealed that there were no significant differences in the expression of *Lmna* between the 5%- and 15%-CS groups at 6, 12, and 24 hours (Figure 2A). This finding indicated that pathological cyclic stretch may not change the transcription of lamin A/C.

Furthermore, we explored the effects of autophagy, a mechano-responsive protein degradation mechanism<sup>22,23</sup> that is involved in lamin B degradation,<sup>24</sup> on lamin A/C

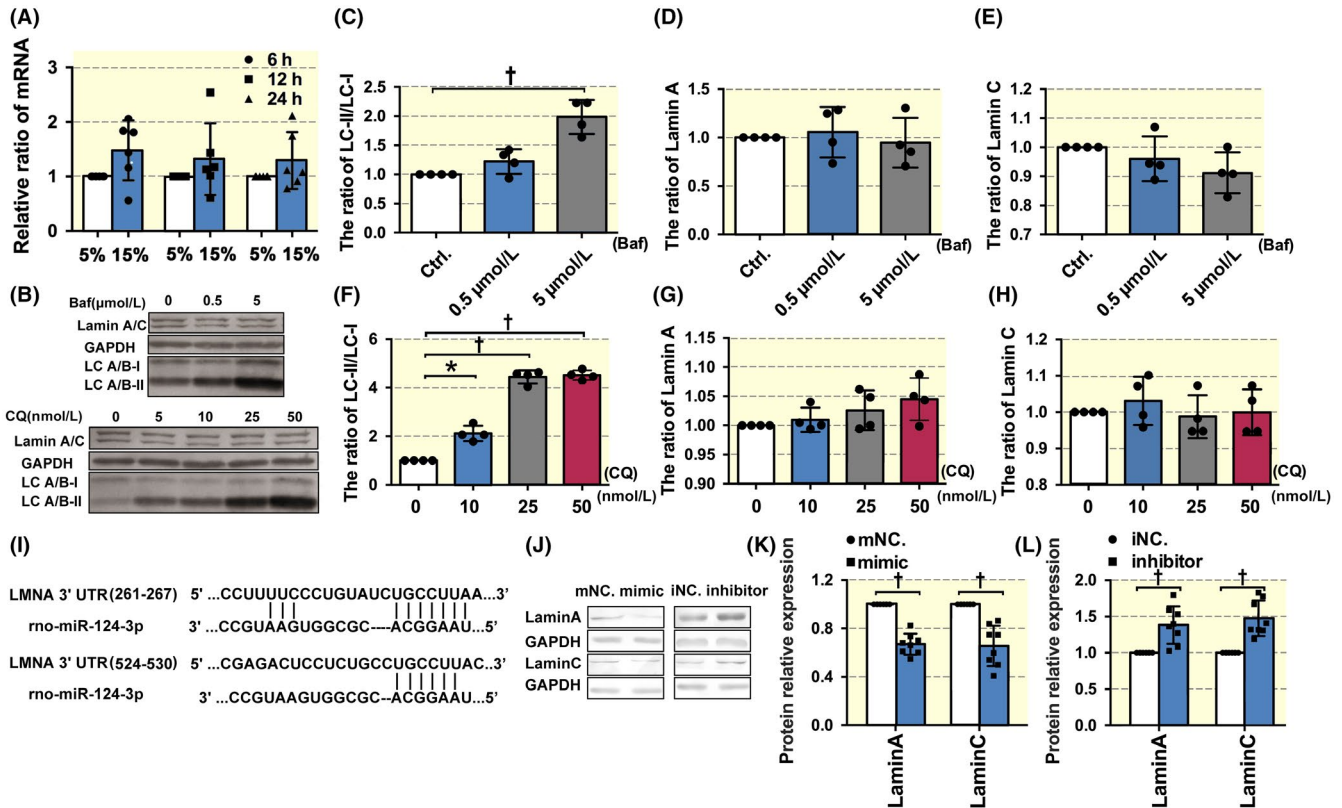


**FIGURE 2** The protein expression of lamin A/C was regulated by miR-124-3p but not by transcription or autophagy. A, Compared with 5%-CS, 15%-CS had little effect on the expression of *lmna*, the mRNA of lamin A/C, at 6, 12, and 24 hours. B, C, D and E, The western blot results indicated that in VSMCs, Baf strongly blocked autophagy level (LC-II/LC-I, C), but had little effect on the expression of lamin A/C (D, E) compared with the control. F, G and H, The western blot results indicated that in VSMCs, CQ greatly induced autophagy (LC-II/LC-I, F), and had little effect on the expression of lamin A/C (G, H) compared with the control. (I) Sequence alignment between rno-miR-124-3p and its putative binding sites in the rat *Lmna* 3'UTR. (J, K, L) The western blot results indicated that in VSMCs, miR-124-3p mimics greatly reduced the protein expression of lamin A/C (K), while miR-124-3p inhibitor greatly increased it compared with the NC (L). The values represent the mean  $\pm$  SD. \* $P < .05$ , † $P < .01$  vs. control. The control value (for A, 5%-CS was used as the control; for B-H, the control was the untreated group; for K, the control was the negative control for miRNA mimics; and for L, was the negative control for miRNA inhibitor) was standardized to 1 ( $n = 4-8$ )

expression. Two kinds of autophagy inhibitors, Baf and CQ, considerably blocked the autophagy in VSMCs (Figure 2B,C,F), but had no significant effect on the protein expression of lamin A/C (Figure 2D,E,G and H). Then, we detected the possible post-transcriptional regulatory mechanism of the expression of lamin A/C.

## 2.4 | miR-124-3p decreases the expression of lamin A/C

MiRs are important endogenous non-coding RNA molecules that negatively regulate protein expression by targeting specific mRNAs and induce their degradation or translational repression. To identify possible miRs in lamin A/C regulation, three online databases, PicTar (<http://www.pictar.org/>), TargetScan (<http://www.targetscan.org/>) and miRanda (<http://www.microrna.org/>) were searched. The search results revealed that there were

two predicted binding sites for miR-124-3p in the *Lmna* 3'UTR (Figure 2I), indicating that miR-124-3p may negatively regulate lamin A/C protein expression. The sequence alignment between miR-124-3p and *Lmna* 3'UTR was well conserved among different species (Table S2). Interestingly, miR-124-3p also targets emerin, another nucleoskeletal protein that was affected by 15%-CS (Figure S2A), and miR-124-3p is important to VSMCs under different pathological states.<sup>25-27</sup>

Subsequently, miR-124-3p was overexpressed or knocked down in VSMCs with a specific mimic or inhibitor respectively. The western blot analysis results indicated that the miR-124-3p mimic significantly reduced the protein expression of lamin A/C (Figure 2K), whereas the inhibitor increased lamin A/C levels compared with the respective NC (Figure 2L). These results indicated that miR-124-3p played an important role in the regulation of lamin A/C expression.



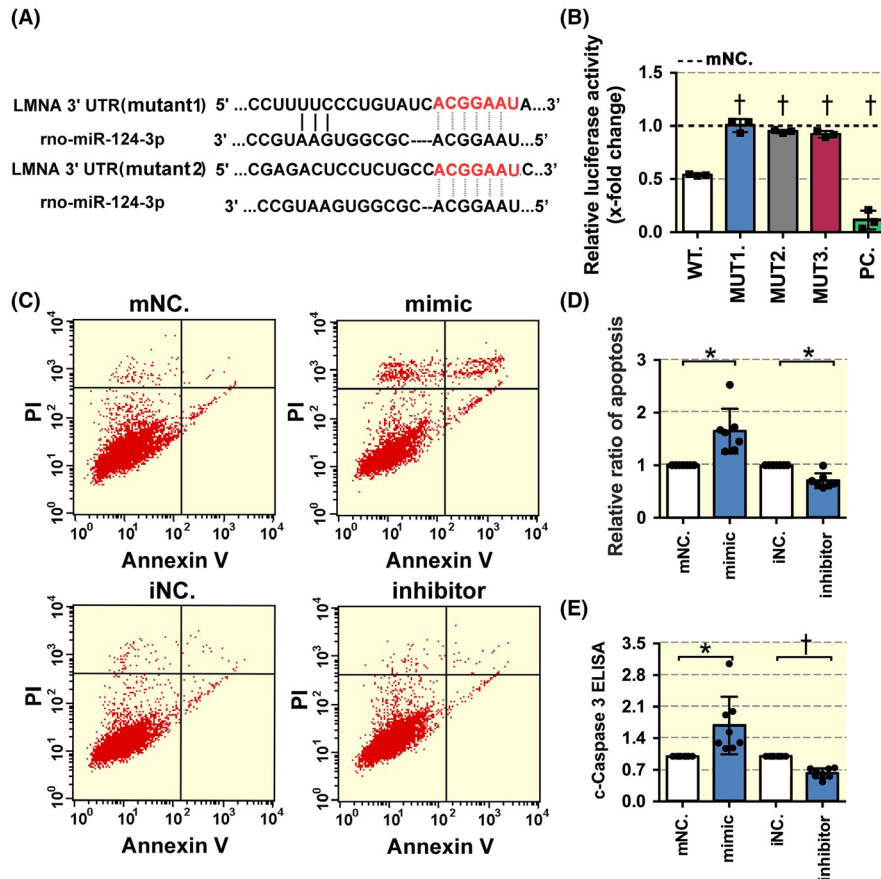


**FIGURE 3** MiR-124-3p has two binding sites in the Lmna 3'UTR. A, Three mutants of the binding sites on the Lmna 3'UTR were created from two mutations at separate sites. B, A dual luciferase reporter gene system was used to detect the luciferase activity in wild-type (WT) and mutant (Mut) Lmna 3'UTR in negative control (NC)- and miR-124-3p mimic-treated HEK-293T cells. miR-124-3p significantly reduced the luciferase activity of the wild-type Lmna 3'UTR in comparison with the Mut Lmna 3'UTR with three culture repeats. C and D, Increasing or suppressing of the expression of miR-124-3p in the VSMCs increased or decreased apoptosis respectively, as detected with AnnexinV-FITC/PI staining. E, Increasing or suppressing of the expression of miR-124-3p in the VSMCs increased or decreased apoptosis respectively, as revealed by cleaved Caspase 3. The values represent the mean  $\pm$  SD. \* $P < .05$ ,  $^{\dagger}P < .01$  vs. control. The control value (for C-E, respective negative control for miRNA mimics and inhibitor was used as the control) was standardized to 1 ( $n = 8$ )

## 2.5 | MiR-124-3p has two binding sites in the 3'UTR of Lmna

A dual luciferase reporter gene system was then used to assess the binding and inhibitory capacity of miR-124-3p to two independent target sites of Lmna 3'UTR. Three Lmna 3'UTR mutants were designed: two with mutations at either target site (Figure 3A), and one with mutations at both sites simultaneously (Table S3). Figure 3B showed that compared with the NC cotransfected, miR-124-3p mimic cotransfected with the wild-type 3'UTR of Lmna significantly decreased the luciferase activity in the HEK-293T cells. In contrast, miR-124-3p cotransfected with the three mutants significantly increased luciferase activity compared with miR-124-3p cotransfected with the wild-type 3'UTR. This suggested that both targeting sites in the 3'UTR of Lmna are important in downregulating the expression of lamin A/C protein by miR-124-3p.

The effect of miR-124-3p on VSMC apoptosis was then examined. Using miR-124-3p mimic or inhibitor, Annexin V/PI and cleaved Caspase 3 ELISA assays revealed that compared with the respective controls, apoptosis of VSMCs was significantly accelerated by the miR-124-3p mimic, but attenuated by the inhibitor compared with the respective controls (Figure 3C,D and E). The above results indicate that miR-124-3p negatively regulated the expression of lamin A/C by targeting two sites on the Lmna 3'UTR, and subsequently promoted the apoptosis of VSMCs.

## 2.6 | The Lamin A/C expression and VSMC apoptosis caused by cyclic stretch are reversed by the inhibition of miR-124-3p

We then explored whether miR-124-3p was mechanically sensitive and whether it participated in the regulation of lamin A/C expression and VSMC apoptosis during cyclic

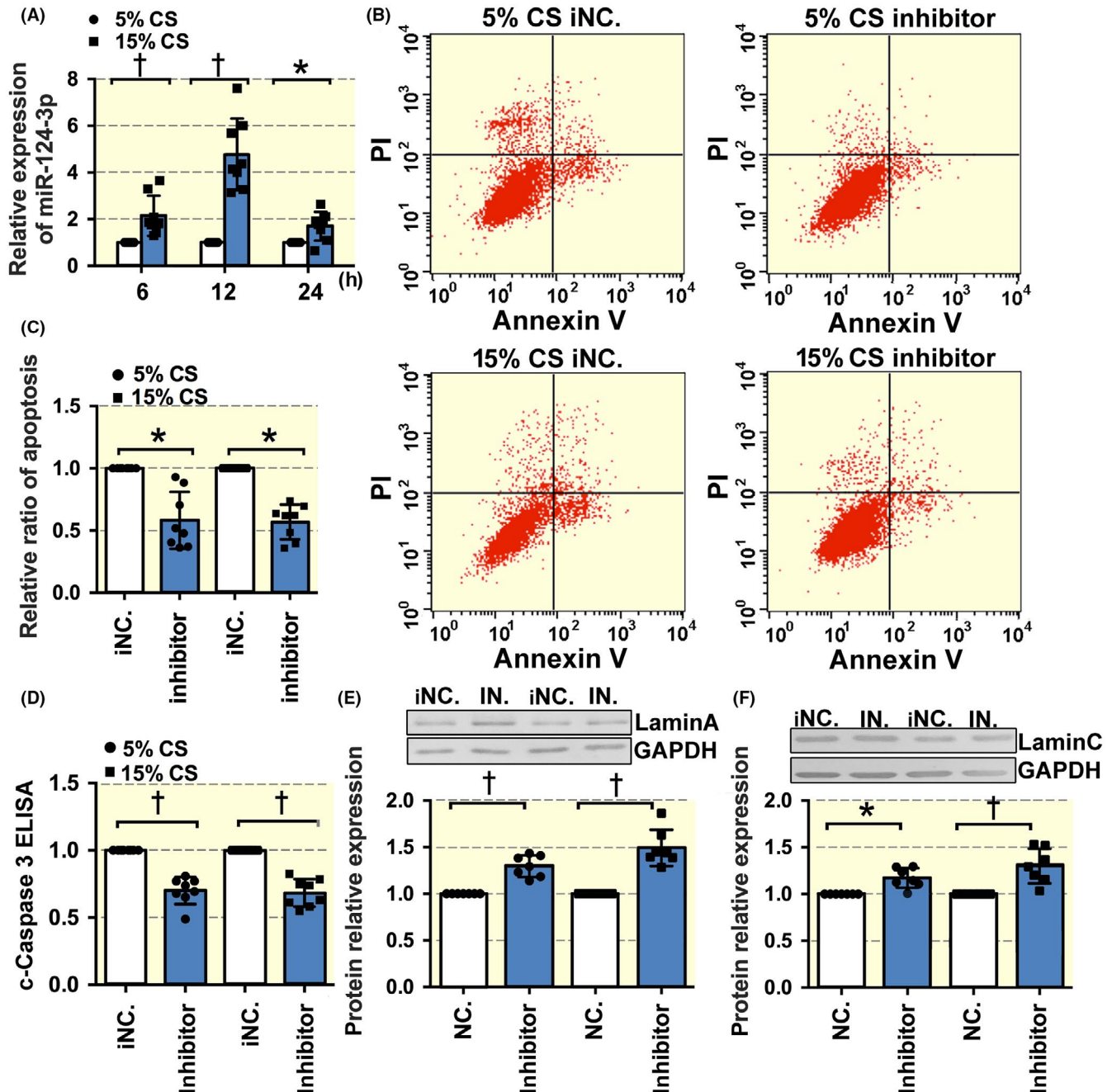


**FIGURE 4** The lamin A/C and apoptosis change caused by cyclic stretch can be reversed by inhibiting miR-124-3p. A, The real-time RT-PCR results revealed that miR-124-3p expression (normalized to U6 expression) was markedly increased in the 15%-CS group compared with the 5%-CS group. B and C, Suppression of the expression of miR-124-3p in the 15%-CS group or the 5%-CS group decreased apoptosis, as revealed by Annexin V/PI staining. D, Suppression of the expression of miR-124-3p in the 15%-CS group or the 5%-CS group decreased apoptosis, as revealed by cleaved Caspase 3 levels. E and F, Suppression of the expression of miR-124-3p in the 15%-CS group or the 5%-CS group increased the expression of lamin A/C. The values represent the mean  $\pm$  SD. \* $P < .05$ , † $P < .01$  vs. control. The control value (for A, 5%-CS was used as the control and for B-F, the inhibitor negative control was used) was standardized to 1 (n = 8)

stretch application. Compared with exposure to 5%-CS, exposure to 15%-CS for 6, 12 and 24 hours markedly increased the expression of miR-124-3p (Figure 4A), which suggested that miR-124-3p was also a mechanosensitive molecule. Compared with the NC control, miR-124-3p inhibitor decreased the apoptosis of VSMCs under both

5%- and 15%-CS conditions (Figure 4B,C,D), while it increased the protein expression of lamin A/C (Figure 4E,F).

These results demonstrated that the miR-124-3p-lamin A/C pathway participates in VSMC apoptosis promoted by 15%-CS.

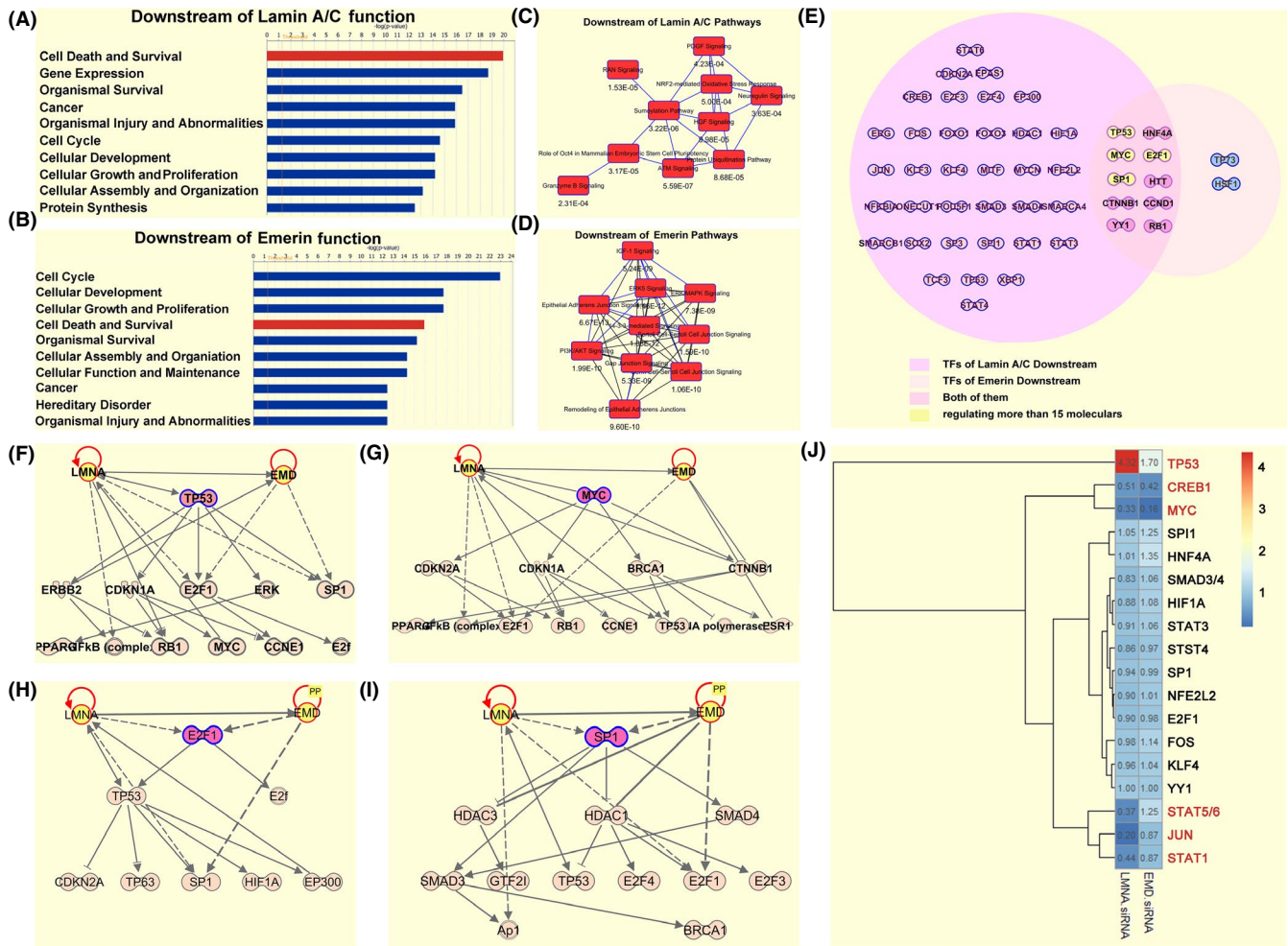


**FIGURE 5** Downregulation of lamin A/C regulated the activation of TFs in VSMCs. A, B, C and D, The functional analysis tool of the IPA software was used to obtain the transcription factor functions and showed that lamin A/C- and emerin-interacting TFs are closely related to cell death and survival through many cellular signalling pathways. E, A total of 48 transcription factors downstream of lamin A/C and emerin are involved in cell death and survival. F, G, H and I, Pathway exploration analysis of several transcription factors that were jointly regulated by lamin A/C and emerin. J, Protein/DNA arrays microarray of various apoptosis-related transcription factor activities predicted by IPA bioinformatics software

## 2.7 | Downregulation of lamin A/C regulates the activation of various TFs in VSMCs

It has been reported that nuclear envelope (NE) proteins regulate DNA synthesis, chromatin organization and gene transcription.<sup>28,29</sup> Therefore, IPA bioinformatics software was used to find the potential downstream transcription factors that may interact with lamin A/C and emerin.

The functional analysis of the software showed that the transcription factors interacting with lamin A/C and emerin were closely related to cell death and survival (Figure 5A,B) through many signalling pathways (Figure 5C,D). As shown in Figure 5E, 48 transcription factors, predicted by IPA to be downstream of lamin A/C and emerin, were involved in cell death and survival. Pathway exploration

was performed to analyse 4 transcription factors that were jointly regulated by lamin A/C and emerin, and these TFs could regulate at least 15 apoptosis-related molecules. We found that the signalling pathways formed by TP53, MYC, E2F1 and SP1 were involved in various stages of apoptosis (Figure 5F-I).

Subsequently, we used a protein/DNA microarray (Panomics Inc, USA) to confirm the effect of lamin A/C or emerin siRNA on the activities of apoptosis-related transcription factors predicted by IPA bioinformatics software (Figure 5J). For six TFs, TP53, CREB1, MYC, STAT5/6, JUN and STAT1, the activation was changed by more than twofold by siRNA of lamin A/C or emerin. These findings suggested that lamin A/C and emerin could modulate the activities of TFs that might participate in the regulation of VSMC apoptosis.



## 2.8 | Hypertension induces the expression of miR-124-3p and represses the expression of lamin A/C in vivo

Using an abdominal aorta coarctation hypertensive model, changes in VSMCs were explored in vivo. At 1 week after surgery, systolic and diastolic blood pressure and mean arterial pressure increased significantly in the hypertensive model (Figure 6B,C). In the thoracic aorta, the wall thickness was markedly increased in hypertensive rats compared with the sham-operated controls by haematoxylin-eosin stain analysis (Figure 6A,D). qPCR and in situ FISH revealed a significant increase in miR-124-3p in the thoracic aorta in the model group (Figure 6F), and this increase was mainly in VSMCs (Figure 6I). Cleaved Caspase 3 ELISA analysis showed that cell apoptosis in the thoracic aorta was also markedly increased in hypertensive rats (Figure 6E), while lamin A/C expression was significantly suppressed (Figure 6G-H).

These results suggested that miR-124-3p/lamin A/C may participate in the abnormal cyclic stretch induced apoptosis of VSMCs caused by hypertension.

## 3 | DISCUSSION

Lamins are type V intermediate filament proteins that form the nuclear lamina, a filamentous network underlying the

inner nuclear membrane of eukaryotic cells.<sup>30</sup> Mutation,<sup>31</sup> aberrant splicing<sup>32</sup> and abnormal expression<sup>33</sup> of lamin A/C, the nuclear A-type lamins, will lead to the disruption of various crucial cellular functions and result in a number of devastating diseases. For example, in the cardiovascular system, mutation of lamin A/C caused by *Lmna* mutations participates in up to 10% of dilated cardiomyopathies (DCMs) and underlies a spectrum of other diseases including muscular dystrophy, lipodystrophy and acrogeria syndromes.<sup>34</sup> Progerin, a truncated and toxic prelamins A caused by aberrant splicing, is associated with severe cardiovascular problems, including cardiac electrical defects, vascular calcification and stiffening, atherosclerosis, myocardial infarction, and stroke, as well as with premature death.<sup>35</sup> In addition, abnormal expression of lamin A/C has also been reported in cardiovascular diseases such as hypertension,<sup>7,33</sup> which leads to dysfunction of vascular cells and leads to vascular remodelling.

However, the mechanisms of how lamin A/C changes cell function have still not conclusively determined. Studies have revealed that the nuclear structural changes caused by lamin A are important to a range of cellular functions. Lamin A is rate-limiting in the 3D migration of diverse cells, including glioma and primary mesenchymal stem cells (MSCs).<sup>36</sup> Harada et al reports that the high ratio of lamin A to lamin B caused by extruded nuclear

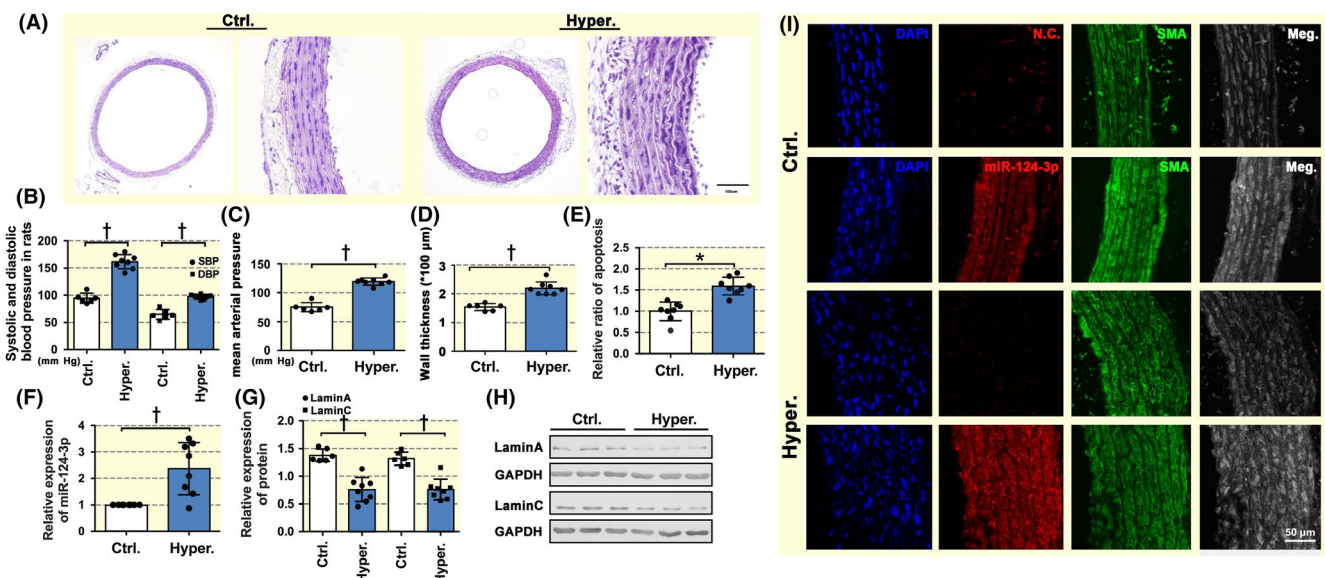


**FIGURE 6** Hypertension induces the expression of miR-124-3p and represses the expression of lamin A/C in vivo. A, After abdominal aorta coarctation for 1 week, haematoxylin-eosin staining was used to analyse the morphological changes in rat thoracic aortas. Scale bar = 100 μm. B-C, The operated rats exhibited markedly higher levels of systolic and diastolic blood pressure and mean arterial pressure than the sham rats. D, The thickness of thoracic aorta wall was increased greatly. E-F, Marked increases of miR-124-3p and apoptosis were detected in the thoracic aorta. (G-H) Lamin A/C expression in the thoracic aortas of hypertension model rats was suppressed as compared with the sham-operated controls. (I) MiR-124-3p and miR-124-3p negative control probe was hybridized in situ FISH. Negative control probe with no known homology to rat genes. The expression of miR-124-3p was markedly increased. Scale bar = 50 μm. The values represent the mean ± SD. \* $P < .05$ , † $P < .01$  vs control. For B-E and G, sham-operated controls were used as a control; for F, a pair of experimental groups and sham-operated control rats were randomly selected for comparison of expression by the  $2^{-\Delta\Delta CT}$  method ( $n = 6-8$ )



shapes after migration, promotes survival against migration-induced stresses.<sup>36</sup> The absence of another kind of nuclear envelope protein, emerin, is also reported to cause abnormal nuclear shape and increase apoptosis in mouse embryonic fibroblasts.<sup>37</sup> Aside from changes in nuclear structure, recent studies have provided support for a role of lamin A in gene regulation. Ho et al reports that lamin A/C-deficient (*Lmna*<sup>-/-</sup>) cells impair nuclear translocation of megakaryoblastic leukaemia 1 (MKL1), a mechanosensitive transcription factor that is pivotal in cardiac development and function.<sup>38</sup> Altered nucleo-cytoplasmic shuttling of MKL1 is caused by altered stress fibre assembly and then affects the differentiation of VSMCs via the RhoA/MKL1/SRF<sup>39</sup> and MYOCD/MYOSLID/MKL1<sup>40</sup> pathways. Under the mechanical stress situation, low shear stress suppresses the expression of lamin A, which subsequently modulates the activation of important transcription factors, eg, Stat-1, Stat-3, Stat-5 and Stat-6, and eventually leads to EC dysfunction.<sup>17</sup> Furthermore, our results demonstrated that knockdown of lamin A/C and emerin changed the activity of a variety of apoptosis-related transcription factors, which may in turn affected apoptosis of VSMCs.

Under hypertension, the repression of lamin A/C has been shown to be a potential biomarker that is associated with blood pressure changes.<sup>33</sup> Maggi et al also reports that abnormalities in lamin A/C cause hypertension.<sup>41</sup> On the other hand, abnormally elevated blood pressure can decrease the expression of lamin A/C in vascular cells. Our results showed that in hypertension, miR-124-3p was involved in the negative regulation of lamin A/C expression. There are many other factors that also affect the expression of lamin A/C. For example, in fibroblast cells, autophagy mediates the degradation, but not the transcription, of lamin A/C proteins during oncogene-induced senescence.<sup>42</sup> The Akt pathway modulates both prelamin A and lamin A degradation in interphase cells.<sup>43</sup> In VSMCs, the ubiquitin degradation pathway also participates in lamin A/C protein reduction.<sup>7</sup> These results suggested that post-transcriptional regulation, including negative regulation by miR-124-3p and protein degradation, play an important role in the protein expression of lamin A/C.

In addition to the effects on transcription factor activity, lamin A/C changes can affect the expression of other nucleoskeletal proteins. Jan et al reports that in lamin C-only (*Lmna*<sup>(LCO/LCO)</sup>) embryonic fibroblasts, the expression of lamin B2 is significantly increased, and there is a trend toward increased levels of lamin B1.<sup>44</sup> In addition, our previous research revealed that transfection of lamin A/C siRNA into VSMCs represses the expression of emerin; in addition, interestingly, emerin siRNA also decreases the expression of lamin A/C.<sup>7</sup> In our study, we proved that a miR-124-3p mimic inhibited the expression of both lamin A/C and emerin, while the dual luciferase reporter assay revealed that the mimic of miR-124-3p could not bind to the Emd 3' UTR (Figure S2F-G).

Therefore, in stress situations, changes in emerin protein were probably caused by changes in lamin A/C expression.

In this research, Flexcell FX5000T Strain Unit was used for the mechanical stretch application *in vitro*. The magnitude of cyclic stretch (5% mimics the physiological cyclic strain, and 15% mimics the pathologically increased cyclic strain) is based on the published clinical ultrasound data which revealed that large artery dilates as much as 15%-CS in hypertension,<sup>45,46</sup> and 5%-CS in normotension.<sup>47,48</sup> Although these magnitudes have been used in our lab<sup>7,49</sup> and other researches<sup>50,51</sup> to demonstrate the roles of mechanical cyclic stretch in vascular remodelling in hypertension, the mechanical situation is highly complex especially in chronic hypertension which is combined with the remodelling of arteries. During acute hypertension or the initiation of arterial hypertension, the distension of blood vessels is increased which has been proved to be an important inducer for the subsequent vascular remodelling.<sup>52,53</sup> If the pathological factors of hypertension are persistent and chronic, arterial walls undergo continuous remodelling that involves VSMC hypertrophy and hyperplasia, and enhances collagen decomposition and reorganization of extracellular matrix, which gradually results in thickening and stiffening of arterial walls.<sup>54</sup> Then the mechanical situation including the changes of stiffness and cyclic stretch will be more complex. Furthermore, because of the limitation of the instrument, the Flexcell FX5000 System could not reach the magnitude of 15%-CS under the rat cardiac cycle. The frequency used in this study simulates the adult human heart rate of 60-100 beats ([www.heart.org](http://www.heart.org)). The mechanobiological mechanism of the above dynamic complex processes remains to be further demonstrated in the future studies.

In summary, this study has revealed that the NE proteins lamin A/C were mechanosensitive molecules in VSMCs. Pathologically elevated cyclic stretch suppressed the expression of lamin A/C by upregulating miR-124-3p, which may subsequently modulate the activation of different TFs and ultimately affect the apoptosis of VSMCs. These results provided evidence that cyclic stretch regulated VSMC functions through an NE protein-mediated mechanism and shed light on the role of nucleoskeletal proteins in mechanotransduction.

## 4 | MATERIALS AND METHODS

### 4.1 | Hypertensive rat model

The animal care and experimental protocols were in accordance with the Animal Management Rules of China (55, 2001, Ministry of Health, China), and the study was approved by the Animal Research Committee of Shanghai Jiao Tong University.

Renal hypertensive rats were generated by abdominal aortic coarctation.<sup>55</sup> Male Sprague-Dawley rats with an average weight of 200 g were randomly assigned to an abdominal

aorta constriction group and a sham surgery control group. All animals were anaesthetized with isoflurane inhalation and treated in sterile conditions. The abdomen was opened, and the abdominal aorta was surgically dissected from the inferior vena cava at a site just above the renal arteries. A 0.8 mm blunt needle was then placed along the side of the isolated aorta segment. Thereafter, a 3-0 suture was tightly tied around the aorta and the overlying needle. The needle was then removed, which caused aortic constriction above the renal arteries. The animals assigned to the control group underwent the same procedure, but without actual ligation of the aorta.

The animals were then observed for 1 week. Before the samples were harvested, blood pressure was measured directly via a carotid cannula method.<sup>55,56</sup> The animals were anaesthetized with isoflurane, and the left carotid artery was catheterized with a 1.1 mm indwelling needle. Blood pressure was monitored directly via the arterial intubation; the transducer was connected to a multiple-lead physiologic recorder (MP30; Biopac Systems, Goleta, CA, USA). Mean arterial pressure was calculated as follows: mean arterial pressure = (systolic blood pressure + 2 × diastolic blood pressure)/3.

## 4.2 | Cell culture

Primary VSMCs were cultured from the medial portions of thoracic aortas from normal male Sprague-Dawley rats after the removal of the adventitia and endothelium. The media of the aorta was isolated surgically and minced into small pieces, which were plated onto 25-cm<sup>2</sup> culture flasks for culture in Dulbecco's Modified Eagle Medium (DMEM, Gibco, USA) containing 10% heat-inactivated fetal bovine serum (FBS, Gibco, Australia), 100 U mL<sup>-1</sup> penicillin and 100 µg mL<sup>-1</sup> streptomycin and were incubated at 37°C in a humidified incubator (95% air and 5% CO<sub>2</sub>). The VSMC monolayers were passaged every 3-4 days after trypsinization, and the cells in passages 6-9 were used for experiments. We used different rat-derived VSMCs for each independent experiment. The purity of VSMCs was examined by using immunofluorescence staining of VSMC specific marker, smooth muscle  $\alpha$ -actin (Sigma-Aldrich, SL, USA, Fig. S1), and a purity more than 95% was used in this study.

## 4.3 | Cyclic stretch application

VSMCs were seeded on flexible silicone-bottom plates (Flexcell International, Hillsborough, NC) at a density of  $2 \times 10^5$  cells per well and incubated overnight in an incubator. After the cells had completely adhered, serum-free medium was used for 24 hours to synchronize the cells. The cells were then exposed to cyclic stretch provided by a FX-5000T Strain Unit (Flexcell International) with an elongation magnitude

of 5%,<sup>47,48</sup> which mimics the physiological cyclic strain in vivo, or 15%,<sup>45,46</sup> which mimics the pathologically increased cyclic strain, at a consistent frequency of 1.25 Hz.

## 4.4 | Autophagy analysis

VSMCs were seeded into 6-well cell culture plates at a density of  $2 \times 10^5$  cells. After the cells had completely adhered, serum-free medium was used for 24 hours to synchronize the cells. Then, increasing concentrations of bafilomycin A1 (Santa Cruz Biotechnology, Dallas, TX, USA, 0, 0.5 and 5 µM respectively) and chloroquine (Sigma-Aldrich, SL, USA, 0, 10, 25 and 50 nM respectively) were added to the medium (Gibco, USA), and the cells were cultured for another 24 hours.

## 4.5 | RNA extraction and SYBR Green Real-Time PCR assay

Total RNA was extracted using TRIzol reagent (Invitrogen, Carlsbad, CA, USA). Optimization reactions consisting of different annealing temperatures and different primer concentrations were performed to determine the most appropriate annealing temperature and primer concentration. Negative controls were run with each experiment. Real-time RT-PCR was performed using a Quanti-Tect SYBR Green PCR Kit (Bio-Rad, Hercules, CA, USA) with 1 µL of cDNA using an iCycler (Bio-Rad, Hercules, CA, USA). Amplification of target genes and the reference gene (U6 for miR expression and GAPDH for Lmna expression) was performed in triplicate, and the PCR products were verified via melt curve analysis. The results were normalized to the reference gene, and the relative gene expression was measured using the  $2^{-\Delta\Delta CT}$  method.

## 4.6 | Western blotting

VSMCs were gently washed with cold PBS and were lysed at 4°C for 5 minutes with lysis buffer (0.15 M Tris, pH 6.8; 1.2% SDS; 15% mercaptoethanol). Lysates were subjected to electrophoretic separation by 10% SDS-PAGE and transferred to nitrocellulose membranes (Hybond, Amersham). Western blot analysis was performed using antibodies directed against lamin A/C, (lamin A/C (1:500) (Santa Cruz Biotechnology, Dallas, TX, USA), lamin A (1:500) (Abcam, Cambridge, UK), lamin C (1:500) (Abcam, Cambridge, UK), emerin (1:500) (Abcam, Cambridge, UK), LC A/B (1:500) (Abcam, Cambridge, UK) and GAPDH (1:500) (Santa Cruz Biotechnology, Dallas, TX, USA). After incubation with alkaline phosphatase-conjugated secondary antibodies (Jackson ImmunoResearch Laboratories, WestGrove, PA, USA), the signals were visualized using nitroblue tetrazolium/bromo-chloroindolyl phosphate (Bio Basic, Markham, ON, Canada), and quantified with Image Studio Digits Ver 5.0 (LI-COR).

#### 4.7 | Transfection with miRs mimics, miR inhibitor or Lmna siRNA

For the transfection experiment, VSMCs were transfected with 100 nmol L-1 rno-miR-124-3p mimic, rno-miR-124-3p inhibitor, Lmna siRNA or the respective negative controls (Gene-Pharma, China). VSMCs were seeded into 6-well cell culture plates at a density of  $2 \times 10^5$  cells. After an 8-hour incubation to allow for attachment, the cells were transfected with Lipofectamine™ 2000 (Invitrogen, Carlsbad, CA, USA) and mimics/inhibitors/siRNAs according to the manufacturer's instructions. Briefly, 100 nmol of siRNAs and 5  $\mu$ L of Lipofectamine™ 2000 were diluted in serum- and antibiotic-free Opti-MEM (Invitrogen, Carlsbad, CA, USA) to a final volume of 800  $\mu$ L. After mixing for 20 minutes at room temperature, the mixture was added dropwise onto the cells, and the cells were incubated at 37°C in a humidified CO<sub>2</sub> incubator. Non-silencing siRNA with no known homology to rat genes was synthesized as a negative control (NC). The sequences of the RNA oligos are listed in Table S1.

#### 4.8 | Dual luciferase reporter assay

The conserved miR-124-3p-binding sequences in the 3' untranslated regions (UTRs) of Lmna, Emd (mRNA of emerin, another nucleoskeletal protein) and the mutation of the binding sequences were all obtained by gene synthesis, and then inserted into the downstream of the luciferase reporter gene (psiCheck-2; Promega, Madison, WI, USA) respectively. To determine the suppression efficiency of miR-124-3p, human HEK-293T cells were transfected with the reporter plasmid or the mutated vectors together with miR-124-3p mimic and NC. Twenty-four hours later, firefly and renilla luciferase activities were measured consecutively by using a dual luciferase reporter assay system (Promega, Madison, WI, USA).

#### 4.9 | Apoptosis assay

Two methods were used to detect the apoptosis of VSMCs, AnnexinV/PI assay and the cleaved Caspase 3 ELISA. AnnexinV-FITC/PI kit (Roche Diagnostics, Germany) was used according to the manufacturer's instructions. Briefly, cells were collected and washed twice with PBS. After being gently resuspended in AnnexinV binding buffer, the cells were incubated with AnnexinV-FITC/PI in the dark for 10 minutes and analysed using flow cytometry using a FACSCalibur (Becton, Dickinson and Company, USA). In the scatter diagrams of the FACS assay, the x-axis represents annexinV-FITC fluorescence and the y-axis depicts PI fluorescence. The upper right quadrant indicates late apoptotic cells, the lower right quadrant indicates early apoptotic cells and the lower left quadrant shows living cells. According to the manufacturer's instructions, the entire right region is defined as apoptotic cells.

Since AnnexinV/PI assay could not exactly distinguish between necrosis and apoptosis, the cleaved Caspase 3 ELISA method, which detected the apoptosis-specific activation of cleaved Caspase 3 (Asp175), was also used to further validate the levels of apoptosis. For in vivo and in vitro assays, the cleaved Caspase 3 ELISA kit (Cell Signaling Technology, Danvers, MA, USA) was used according to the manufacturer's instructions. VSMCs were treated with lysis buffer (with 1 mM PMSF freshly added) on ice. The lysates were transferred to appropriate tubes and then centrifuged for 10 minutes at 14 000 rpm and 4°C. The samples were sequentially incubated with relevant antibodies according to the instructions mentioned on the cleaved Caspase 3 ELISA kit. The absorbance at 450 nm was measured using an ELISA plate reader (Bio-Rad 680).

#### 4.10 | Ingenuity pathway analysis

The possible biological processes and functional classifications of the target transcription factor of lamin A/C and emerin were obtained with Ingenuity Pathway Analysis (IPA) software (Qiagen) (<https://www.qiagenbioinformatics.com/products/ingenuity-pathway-analysis> content version: 39 480 507). IPA integrated the available knowledge on genes, drugs, chemicals, protein families, processes and pathways based on the interactions and functions derived from the Ingenuity Pathways Knowledge Database Literature. IPA was used to understand the complex biological and chemical systems at the core of life science research based on lectures or predicated analysis.<sup>57</sup>

#### 4.11 | Protein/DNA array analysis

To detect the activities of transcription factors induced by lamin A/C and emerin interference, a protein/DNA array was used. Nuclear proteins were prepared from VSMCs transfected with siRNA by using a nuclear extraction kit (Panomics, USA) following the manufacturer's instructions. TranSignal Protein/DNA Array I kit (Panomics, USA) was used to identify the DNA-binding properties of 18 transcription factors (TFs) predicted by IPA. In general, nuclear extracts from ECs were incubated with TranSignal probe mix (Panomics) containing 18 biotin-labelled double-stranded DNA oligonucleotides for 30 minutes at 15°C. The biotin-labelled oligonucleotides that were specifically bound to the TFs were eluted and hybridized to a TranSignal array membrane containing oligonucleotides. The blots were then washed and incubated with horseradish peroxidase (HRP)-conjugated streptavidin according to the manufacturer's instructions. The hybridization signals on the array were detected using standard chemiluminescence procedures with Hyperfilm ECL (2-10 minutes). The relative spot intensities were determined using ScanAlyze software to obtain numerical data for comparisons.



#### 4.12 | Haematoxylin-Eosin staining

The thoracic artery samples were frozen-sectioned into 6  $\mu\text{m}$  sections. The sections were then stained with haematoxylin for 8 minutes and rinsed with distilled water, and 0.1% hydrochloric acid in 70% ethanol. After rinsing with tap water for 5 minutes, 0.3% ammonium hydroxide was used for 5 minutes. The slides were then rinsed with 70% and 90% ethanol for 5 minutes respectively, stained with eosin for 30 s and rinsed again with distilled water. Increasing concentrations of ethanol (70%, 90%, 95% and 100%) were then used for dehydration, followed by xylene twice. The raw data were analysed with ImageJ (Rawak Software, Inc, Germany).

#### 4.13 | FISH analysis

The thoracic artery samples were plunged into freezing isopentane and frozen-sectioned into 6- $\mu\text{m}$  sections. To block endogenous peroxidase activity, the sections were treated with 0.3%  $\text{H}_2\text{O}_2$  before acetylation in acetic anhydride-triethanolamine and washed in  $2 \times$  saline sodium citrate (SSC) and PBS before permeabilization with proteinase K (5 mg mL<sup>-1</sup>). The thoracic artery sections were then hybridized with a miR-124-3p biotinylated probe or a negative control biotinylated probe (Shanghai GenePharma, Shanghai, China) (200 nM) overnight at 56°C. After five post-hybridization washes in SSC at room temperature, a wash in 50% formamide/SSC/0.1% Tween 20 at the hybridization temperature (25°C) and a wash in  $0.2 \times$  SSC at room temperature, the FISH signals were amplified with Tyramide SuperBoost Kits followed by an Alexa Fluor Tyramide Kit (B40933; Thermo Fisher Scientific) and photographed under a microscope (DP70; Olympus). The sequences of the RNA oligos are listed in Table S1.

#### 4.14 | Statistical analysis

Statistical analysis was performed and figures were made with GraphPad Prism 6.0 biochemical statistical package (GraphPad Software, Inc, San Diego, CA). All values were expressed as the mean  $\pm$  SD. Gaussian distribution of values was tested using Kolmogorov-Smirnov test. A paired t test was used for paired data with a Gaussian distribution; Wilcoxon matched-pairs signed rank test was used for paired data not with Gaussian distribution or the sample size was less than 5. Besides, Friedman test was used for multiple comparisons with a single reference group which sample size was  $< 5$ . An unpaired t test was used for the unpaired data with a Gaussian distribution. Differences with values of  $P < .05$  were regarded as statistically significant.

#### CONFLICT OF INTEREST

The authors confirm that there are no conflicts of interest.

#### ACKNOWLEDGEMENTS

This research was supported by grants from the National Natural Science Foundation of China, nos. 11572199 and 11625209.

#### ORCID

Ying-Xin Qi  <https://orcid.org/0000-0002-5428-9749>

#### REFERENCES

1. Lu Y, Zhang L, Liao X, et al. Kruppel-like factor 15 is critical for vascular inflammation. *J Clin Invest*. 2013;123:4232-4241.
2. Sun HJ, Ren XS, Xiong XQ, et al. NLRP3 inflammasome activation contributes to VSMC phenotypic transformation and proliferation in hypertension. *Cell Death Dis*. 2017;8:e3074.
3. Devlin AM, Clark JS, Reid JL, Dominiczak AF. DNA synthesis and apoptosis in smooth muscle cells from a model of genetic hypertension. *Hypertension*. 2000;36:110-115.
4. Liu J, Huang Y, Chen S, Tang C, Jin H, Du J. Role of endogenous sulfur dioxide in regulating vascular structural remodeling in hypertension. *Oxid Med Cell Longev*. 2016;2016:4529060.
5. Chien S. Mechanotransduction and endothelial cell homeostasis: the wisdom of the cell. *Am J Physiol Heart Circ Physiol*. 2007;292:H1209-1224.
6. Haga JH, Li YS, Chien S. Molecular basis of the effects of mechanical stretch on vascular smooth muscle cells. *J Biomech*. 2007;409:47-960.
7. Qi YX, Yao QP, Huang K, et al. Nuclear envelope proteins modulate proliferation of vascular smooth muscle cells during cyclic stretch application. *Proc Natl Acad Sci USA*. 2016;113:5293-5298.
8. Mayr M, Hu Y, Hainaut H, Xu Q. Mechanical stress-induced DNA damage and rac-p38 MAPK signal pathways mediate p53-dependent apoptosis in vascular smooth muscle cells. *FASEB J*. 2002;16:1423-1425.
9. Rodríguez AI, Csányi G, Ranayhossaini DJ, et al. MEF2B-Nox1 signaling is critical for stretch-induced phenotypic modulation of vascular smooth muscle cells. *Arterioscler Thromb Vasc Biol*. 2015;35:430-438.
10. Zhou RH, Lee TS, Tsou TC, et al. Stent implantation activates Akt in the vessel wall: role of mechanical stretch in vascular smooth muscle cells. *Arterioscler Thromb Vasc Biol*. 2003;23:2015-2020.
11. Dai Y, Tian Y, Luo DY, et al. Cyclic stretch induces human bladder smooth muscle cell proliferation in vitro through muscarinic receptors. *Mol Med Rep*. 2015;11:2292-2298.
12. Wedgwood S, Lakshminrusimha S, Schumacker PT, Steinhorn RH. Cyclic stretch stimulates mitochondrial reactive oxygen species and Nox4 signaling in pulmonary artery smooth muscle cells. *Am J Physiol Lung Cell Mol Physiol*. 2015;309:L196-203.
13. Abiko H, Fujiwara S, Ohashi K, et al. Rho-guanine nucleotide exchange factors involved in cyclic stretch-induced reorientation of vascular endothelial cells. *J Cell Sci*. 2015;128:1683-1695.
14. Ma Y, Fu S, Lu L, Wang X. Role of androgen receptor on cyclic mechanical stretch-regulated proliferation of C2C12 myoblasts and its upstream signals: IGF-1-mediated PI3K/Akt and MAPKs pathways. *Mol Cell Endocrinol*. 2017;450:83-93.

15. Wu Y, Zhuang J, Zhao D, Zhang F, Ma J, Xu C. Cyclic stretch-induced the cytoskeleton rearrangement and gene expression of cytoskeletal regulators in human periodontal ligament cells. *Acta Odontol Scand.* 2017;75:507-516.
16. Zielinski A, Linnartz C, Pleschka C, et al. Reorientation dynamics and structural interdependencies of actin, microtubules and intermediate filaments upon cyclic stretch application. *Cytoskeleton (Hoboken).* 2018;75:385-394.
17. Han Y, Wang L, Yao QP, et al. Nuclear envelope proteins Nesprin2 and LaminA regulate proliferation and apoptosis of vascular endothelial cells in response to shear stress. *Biochim Biophys Acta.* 1853;1165-1173:2015.
18. Gruenbaum Y, Medalia O. Lamins: the structure and protein complexes. *Curr Opin Cell Biol.* 2015;32:7-12.
19. Lammerding J, Schulze PC, Takahashi T, et al. Lamin A/C deficiency causes defective nuclear mechanics and mechano-transduction. *J Clin Invest.* 2004;113:370-378.
20. López-Alonso I, Blázquez-Prieto J, Amado-Rodríguez L, et al. Preventing loss of mechanosensation by the nuclear membranes of alveolar cells reduces lung injury in mice during mechanical ventilation. *Sci Transl Med.* 2018;10:eaam7598.
21. Balachandran K, Sucusky P, Jo H, Yoganathan AP. Elevated cyclic stretch alters matrix remodeling in aortic valve cusps: implications for degenerative aortic valve disease. *Am J Physiol Heart Circ Physiol.* 2009;29:H756-764.
22. Ding Z, Liu S, Deng X, Fan Y, Wang X, Mehta JL. Hemodynamic shear stress modulates endothelial cell autophagy: Role of LOX-1. *Int J Cardiol.* 2015;184:86-95.
23. Yeganeh B, Lee J, Bilodeau C, et al. Acid Sphingomyelinase inhibition attenuates cell death in mechanically ventilated newborn rat lung. *Am J Respir Crit Care Med.* 2019;199:760-772.
24. Dou Z, Xu C, Donahue G, et al. Autophagy mediates degradation of nuclear lamina. *Nature.* 2015;527:105-109.
25. Choe N, Kwon DH, Shin S, et al. The microRNA miR-124 inhibits vascular smooth muscle cell proliferation by targeting S100 calcium-binding protein A4 (S100A4). *FEBS Lett.* 2017;591:1041-1052.
26. Tang Y, Yu S, Liu Y, Zhang J, Han L, Xu Z. MicroRNA-124 controls human vascular smooth muscle cell phenotypic switch via Sp1. *Am J Physiol Heart Circ Physiol.* 2017;313:H641-649.
27. Chen W, Yu F, Di M, et al. MicroRNA-124-3p inhibits collagen synthesis in atherosclerotic plaques by targeting prolyl 4-hydroxylase subunit alpha-1 (P4HA1) in vascular smooth muscle cells. *Atherosclerosis.* 2018;277:98-107.
28. Isermann P, Lammerding J. Nuclear mechanics and mechanotransduction in health and disease. *Curr Biol.* 2013;23:R1113-1121.
29. Andrés V, González JM. Role of A-type lamins in signaling, transcription, and chromatin organization. *J Cell Biol.* 2009;187:945-957.
30. Janin A, Bauer D, Ratti F, Millat G, Méjat A. Nuclear envelopathies: a complex LINC between nuclear envelope and pathology. *Orphanet J Rare Dis.* 2017;12:147.
31. Captur G, Arbustini E, Bonne G, et al. Lamin and the heart. *Heart.* 2018;104:468-479.
32. Harhoury K, Navarro C, Depetris D, et al. MG132-induced progerin clearance is mediated by autophagy activation and splicing regulation. *EMBO Mol Med.* 2017;9:1294-1313.
33. Zeller T, Schurmann C, Schramm K, et al. Transcriptome-wide analysis identifies novel associations with blood pressure. *Hypertension.* 2017;70:743-750.
34. Wang X, Zabell A, Koh W, Tang WH. Lamin A/C cardiomyopathies: Current understanding and novel treatment strategies. *Curr Treat Options Cardiovasc Med.* 2017;19:21.
35. Dorado B, Andrés V. A-type lamins and cardiovascular disease in premature aging syndromes. *Curr Opin Cell Biol.* 2017;46:17-25.
36. Harada T, Swift J, Irianto J, et al. Nuclear lamin stiffness is a barrier to 3D migration, but softness can limit survival. *J Cell Biol.* 2014;204:669-682.
37. Lammerding J, Hsiao J, Schulze PC, Kozlov S, Stewart CL, Lee RT. Abnormal nuclear shape and impaired mechanotransduction in emerin-deficient cells. *J Cell Biol.* 2005;170:781-791.
38. Ho CY, Jaalouk DE, Vartiainen MK, Lammerding J. Lamin A/C and emerin regulate MKL1-SRF activity by modulating actin dynamics. *Nature.* 2013;497:507-511.
39. Long X, Cowan SL, Miano JM. Mitogen-activated protein kinase 14 is a novel negative regulatory switch for the vascular smooth muscle cell contractile gene program. *Arterioscler Thromb Vasc Biol.* 2013;33:378-386.
40. Zhao J, Zhang W, Lin M, et al. MYOSLID Is a novel serum response factor-dependent long noncoding RNA that amplifies the vascular smooth muscle differentiation program. *Arterioscler Thromb Vasc Biol.* 2016;36:2088-2099.
41. Patni N, Xing C, Agarwal AK, Garg A. Juvenile-onset generalized lipodystrophy due to a novel heterozygous missense LMNA mutation affecting lamin C. *Am J Med Genet A.* 2017;173:2517-2521.
42. Lenain C, Gussyatiner O, Douma S, van den Broek B, Peeper DS. DS Peeper: Autophagy-mediated degradation of nuclear envelope proteins during oncogene-induced senescence. *Carcinogenesis.* 2015;36:1263-1274.
43. Bertacchini J, Beretti F, Cenni V, et al. The protein kinase Akt/PKB regulates both prelamin A degradation and Lmna gene expression. *FASEB J.* 2013;27:2145-2155.
44. Lammerding J, Fong LG, Ji JY, et al. Lamin A and lamin C but not lamin B1 regulate nuclear mechanics. *J Biol Chem.* 2006;281:25768-25780.
45. Safar ME, Peronneau PA, Levenson JA, Toto-Moukoko JA, Simon AC. Pulsed Doppler: diameter, blood flow velocity and volumic flow of the brachial artery in sustained essential hypertension. *Circulation.* 1981;63:393-400.
46. Williams B. Mechanical influences on vascular smooth muscle cell function. *J Hypertens.* 1998;16:1921-1929.
47. Maul TM, Chew DW, Nieponice A, Vorp DA. Mechanical stimuli differentially control stem cell behavior: morphology, proliferation, and differentiation. *Biomech Model Mechanobiol.* 2011;10:939-953.
48. Asanuma K, Magid R, Johnson C, Nerem RM, Galis ZS. Uniaxial strain upregulates matrix-degrading enzymes produced by human vascular smooth muscle cells. *Am J Physiol Heart Circ Physiol.* 2003;284:H1778-1784.
49. Qi YX, Qu MJ, Yan ZQ, et al. Cyclic strain modulates migration and proliferation of vascular smooth muscle cells via Rho-GDIalpha, Rac1, and p38 pathway. *J Cell Biochem.* 2010;109:906-914.
50. Wernig F, Mayr M, Xu Q. Mechanical stretch-induced apoptosis in smooth muscle cells is mediated by beta1-integrin signaling pathways. *Hypertension.* 2003;41:903-911. <https://doi.org/10.1161/01.HYP.0000062882.42265.88.54>.
51. Kinoshita H, Suzuma K, Maki T, et al. Cyclic stretch and hypertension increase retinal succinate: potential mechanisms for exacerbation of ocular neovascularization by mechanical stress. *Invest Ophthalmol Vis Sci.* 2014;55:4320-4326.

52. Grote K, Flach I, Luchtefeld M, et al. Mechanical stretch enhances mRNA expression and proenzyme release of matrix metalloproteinase-2 (MMP-2) via NAD(P)H oxidase-derived reactive oxygen species. *Circ Res*. 2003;92:e80-86.
53. Langille BL. Remodeling of developing and mature arteries: endothelium, smooth muscle, and matrix. *J Cardiovasc Pharmacol*. 1993;21(Suppl 1):S11-17.
54. Lehoux S, Tedgui A. Signal transduction of mechanical stresses in the vascular wall. *Hypertension*. 1998;32:338-345.
55. Barton CH, Ni Z, Vaziri ND. Enhanced nitric oxide inactivation in aortic coarctation-induced hypertension. *Kidney Int*. 2001;60:1083-1087.
56. Vaziri ND, Zhou XJ, Smith J, Oveisi F, Baldwin K, Purdy RE. In vivo and in vitro pressor effects of erythropoietin in rats. *Am J Physiol*. 1995;269:F838-845.
57. Dai L, Li C, Shedden KA, Misek DE, Lubman DM. Comparative proteomic study of two closely related ovarian endometrioid

adenocarcinoma cell lines using cIEF fractionation and pathway analysis. *Electrophoresis*. 2009;30:1119-1131.

## SUPPORTING INFORMATION

Additional supporting information may be found online in the Supporting Information section at the end of the article.

**How to cite this article:** Bao H, Li H-P, Shi Q, et al. Lamin A/C negatively regulated by miR-124-3p modulates apoptosis of vascular smooth muscle cells during cyclic stretch application in rats. *Acta Physiol*. 2019;e13374. <https://doi.org/10.1111/apha.13374>